Water Resources Research®

RESEARCH ARTICLE
10.1029/2021WR030299

Laboratory Flume and Numerical Modeling Experiments Show Log Jams and Branching Channels Increase Hyporheic Exchange

K. Wilhelmsen[1], A. H. Sawyer[1], A. Marshall[2], S. McFadden[3], K. Singha[3], and E. Wohl[2]

[1]School of Earth Sciences, The Ohio State University, Columbus, OH, USA, [2]Colorado School of Mines, Hydrologic Science and Engineering Program, Golden, CO, USA, [3]Department of Geosciences, Colorado State University, Fort Collins, CO, USA

Key Points:

- Logjams increase stream-groundwater connectivity by increasing hyporheic exchange rates and to a lesser degree, inundated area
- The range of hyporheic flow lengths and residence times increases with jam size and channel complexity
- Jams facilitate more chemical processing in the hyporheic zone, especially at lower stream flows

Supporting Information:

Supporting Information may be found in the online version of this article.

Correspondence to:

A. H. Sawyer,
sawyer.143@osu.edu

Citation:

Wilhelmsen, K., Sawyer, A. H., Marshall, A., McFadden, S., Singha, K., & Wohl, E. (2021). Laboratory flume and numerical modeling experiments show log jams and branching channels increase hyporheic exchange. *Water Resources Research*, *57*, e2021WR030299. https://doi.org/10.1029/2021WR030299

Received 29 APR 2021
Accepted 7 SEP 2021

Abstract Log jams alter gradients in hydraulic head, increase the area available for hyporheic exchange by creating backwater areas, and lead to the formation of multiple channel branches and bars that drive additional exchange. Here, we numerically simulated stream-groundwater interactions for two constructed flume systems—one without jams and one with a series of three jams—to quantify the effects of interacting jam structures and channel branches on hyporheic exchange at three stream flow rates. In simulations without jams, average hyporheic exchange rates ranged from 2.1×10^{-4} to 2.9×10^{-4} m/s for various stream discharge scenarios, but with jams, exchange rates increased to a range of 1.3×10^{-3}–3.5×10^{-3} m/s. Largely due to these increased hyporheic exchange rates, jams increased stream-groundwater connectivity or decreased the turnover length that stream water travels before interacting with the hyporheic zone, by an order of magnitude, and drove long flow paths that connected multiple jams and channel threads. Decreased turnover lengths corresponded with greater reaction significance per km, a measure of the potential for the hyporheic zone to influence stream water chemistry. For low-flow conditions, log jams increased reaction significance per km five-fold, from 0.07 to 0.35. Jams with larger volumes led to longer hyporheic residence times and path lengths that exhibited multiple scales of exchange. Additionally, the longest flow paths connecting multiple jams occurred in the reach with multiple channel branches. These findings suggest that large gains in hydrologic connectivity can be achieved by promoting in-stream wood accumulation and the natural formation of both jams and branching channels.

Plain Language Summary Log jams widen streams, create pools, and cause the stream to branch and follow new paths. These processes affect surface water-groundwater interaction or the exchange between the stream and the water moving within the sediments and streambanks. In this work, we used three-dimensional computer models of an experimental laboratory flume system to understand the effects of multiple log jams and channel branches on this surface water-groundwater interaction. We found that when log jams are present in streams, the rate of water moving between the surface and subsurface is greater than it would be otherwise and increases under flood conditions. Log jams also increase chemical contact with the streambed, which can lead to natural improvements in stream water quality. We also found that where log jams are bigger and located near branching channels, stream water that enters the bed follows diverse pathways that span a wide range of travel distances and times before returning to the stream. Essentially, in-stream wood and channel branching increases water flow in streambed sediments and increases the potential for chemical processing to occur.

1. Introduction

Hyporheic exchange, or mixing between streams and groundwater, is driven by hydraulic head gradients along the streambed, which occur where currents interact with ripples and pool-riffle sequences (Buffington & Tonina, 2009; Gooseff et al., 2006), channel bends (Wondzell et al., 2009), and large wood jams (Beckman & Wohl, 2014; Tonina & Buffington, 2009). The benefits of hyporheic exchange are diverse, including nutrient retention (Crenshaw et al., 2002; Harvey et al., 2013; Valett et al., 1997), pollutant degradation (Gandy et al., 2007), buffering of surface water and streambed temperatures (Arrigoni et al., 2008; Majerova et al., 2015), and the improvement of aquatic habitat (Hester & Gooseff, 2010; Xu et al., 2012). For example,

hyporheic exchange supplies oxygen to shallow sediments where fish embryos and macroinvertebrates dwell and modifies daily temperature fluctuations, impacting invertebrate diversity and hatching times of salmonid eggs (Evans & Petts, 1997).

Large wood is a natural feature in small streams that promotes hyporheic exchange through multiple mechanisms, both direct and indirect (Majerova et al., 2015; Tonina & Buffington, 2009). Directly, structures such as channel-spanning logs and steps increase hydraulic head gradients that drive flow through the bed (Curran & Wohl, 2003; Endreny et al., 2011; Lautz et al., 2006; Sawyer et al., 2011). Indirectly, jams also enhance the magnitude of step-pool and pool-riffle bedforms (Curran & Wohl, 2003; Montgomery & Buffington, 1997) and force anabranching channels (Abbe & Montgomery, 1996; Sear et al., 2010), all of which promote vertical and lateral flow (Buffington & Tonina, 2009; Gooseff et al., 2006; Tonina & Buffington, 2007). Moreover, large wood increases alluvial cover in streambeds that would otherwise have exposed bedrock (Buffington & Tonina, 2009; Faustini & Jones, 2003; Massong & Montgomery, 2000; Montgomery et al., 2003), thus creating a potential region for hyporheic mixing. Under high-flow conditions, jams also retain water in upstream pools and release it from storage through surface and hyporheic flow paths under subsequent low-flow conditions (Nyssen et al., 2011). In summary, reaches with established jam structures are more likely to exhibit greater complexity in head gradients, channel morphology, and streambed sediment cover (Livers & Wohl, 2016; Sear et al., 2010), all of which interact to enhance hyporheic flow.

Due to the morphologic complexity of streams with numerous jams, it can be challenging to quantify hyporheic exchange in the field at relevant scales that span multiple jams and related channel features. Scaled flume experiments offer an alternative approach to understand the effects of log jams and channel morphologic complexity on hyporheic exchange. The flume system can be controlled for substrate properties, surface water discharge, channel planform, and wood presence. Incorporating numerical models makes it possible to analyze hyporheic flow paths within flumes at greater spatial resolution than possible with observations (Endreny et al., 2011; Krause et al., 2011; Salehin et al., 2004; Savant et al., 1987; Tonina & Buffington, 2007). Previous studies have combined flume experiments with numerical models to analyze hyporheic exchange due to relatively simple log-formed structures. Sawyer et al. (2011) examined single, channel-spanning logs and showed that the hyporheic exchange rate scales with the blockage ratio (fraction of channel depth obstructed by the log) and channel Froude number. Endreny et al. (2011) analyzed hydraulic jumps and hyporheic flow around steps and found that hydraulic jumps create heterogeneity in downwelling/upwelling patterns and hyporheic flow paths. They suggested these patterns likely impact the transport of redox-sensitive solutes and biogeochemical conditions within sediments. Fewer controlled flume studies have examined the effects of multiple large wood structures on hyporheic exchange. Mutz et al. (2007) ran experiments with abundant wood and found that greater wood presence alters bedforms and increases flow resistance and vertical exchange, but their flume configuration did not allow for anabranching channels, which are often observed near log jams in the field (Collins et al., 2012; Sear et al., 2010; Wohl, 2011). While these flume studies have shaped our understanding of hyporheic exchange around individual structures and, to some extent, the interactions between structures, an opportunity exists to test the effects of multiple jams and more complex jam-formed channel morphologies on hyporheic exchange patterns and characteristics.

Here, we set out to determine the effects of jam structures, in combination with multithreaded channels, on the hyporheic flow regime of small streams. We integrate high-resolution coupled surface water-groundwater flow models to analyze hyporheic flow in an experimental flume with multiple jams and branching channels. The flume setup is scaled to channel geometry and grain-size attributes of Little Beaver Creek (Doughty et al., 2020), a third-order stream in the Rocky Mountains of Colorado, USA. A related study by Ader et al. (2021) details the effects of in-stream wood on transient storage in Little Beaver Creek. We sought to understand patterns and timescales of exchange around individual jams as well as their collective effect on hyporheic connectivity, measured by turnover length, and potential chemical transformations in the hyporheic zone, determined by the reaction significance factor.

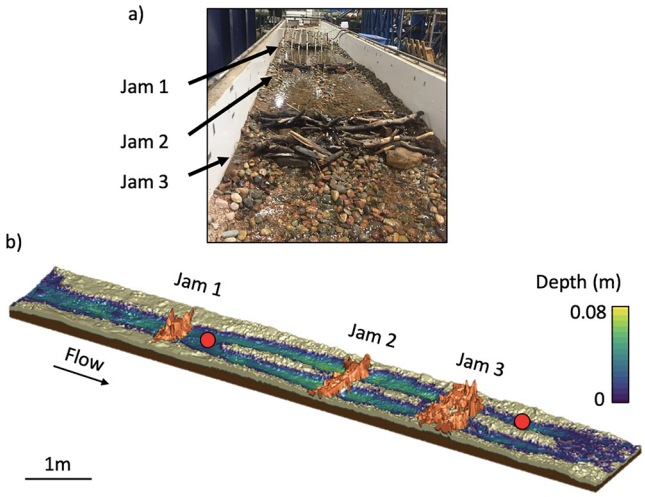

Figure 1. (a) Photo of the flume looking upstream. (b) Digital elevation model, draped with surface water depths simulated under a discharge of 1.4 L/s. Red circles denote locations where fluid electrical conductivity was measured in surface water within the flume and compared with numerical simulations (see Supporting Information S1).

2. Methods

2.1. Flume Setup

The physical flume has an experimental section that is 9.2-m long and 1.2-m wide with a sediment box that is 0.1-m deep. The overall slope of the sediment surface is 0.01 m/m or 1% (Figure 1). The impermeable bottom of the sediment box also has a 1% slope such that the sediment storage depth is relatively constant. This is similar in nature to mountain channels where shallow bedrock constrains the hyporheic zone, though the contact between bedrock and alluvium in natural systems is more complex. Water cascades into the experimental section over a stepped spillway. The sediment in the experimental section is generally composed of a layer of coarse sand and an armored surface layer with gravel and coarse sand. The median grain sizes of the deep layer and surface layer are 2.83 and 12.7 mm, respectively. According to the Shahabi empirical method (Dolzyk & Chmielewska, 2014; Shahabi et al., 1984), hydraulic conductivities are estimated as 8.9×10^{-5} m/s for the deep layer and 2.5×10^{-3} m/s for the armored surface layer, but model-data comparison (Supporting Information S1) and typical hydraulic characteristics of unconsolidated gravel and sand sediments (Freeze & Cherry, 1979) suggest that hydraulic conductivities are likely an order of magnitude greater. The two layers' porosities are estimated at 0.3, typical of unconsolidated fluvial sediments (Freeze & Cherry, 1979).

Three log jams were formed by hand to examine the effects of log jam and channel complexities on hyporheic exchange dynamics (Figure 1). The total volume for each jam (solid wood pieces plus void space) was quantified from the mapped outer surface of the jam in the digital elevation model. The geometry of the base of the jam (or the sediment surface beneath the jam) was known to be flat. From upstream to downstream, Jam 1 is located within a single channel and has a volume of 0.02 m^3, as measured by the total solid and void space occupied by the wood pieces. Jam 2 spans two channel threads and has a volume of 0.04 m^3. Jam 3 spans two channel threads and is a more complex jam structure comprised of multiple, larger wood pieces with a total volume of 0.07 m^3. Given the similar wood materials and difficulty in hand-packing jams in an experimental system, all three jams were estimated to have a porosity of 0.7, the upper limit of the expected range for large wood jams in the field (0.6–0.7) (Spreitzer et al., 2020).

Experiments were conducted under three flow conditions: low-flow (1.4 L/s), medium-flow (4.3 L/s), and high-flow (8.5 L/s). For each run, a conservative salt tracer was injected continuously for two hours, and solute breakthrough curves were monitored with conductivity sensors at multiple locations in surface water every 5.0 s (Figure 1b). The water in the flume was not recirculated: salt tracer exiting the downstream flume extent was not reintroduced to the flume system.

A digital elevation model for the flume was constructed using structure from motion. Images were captured at regular downstream intervals with a camera mounted at consistent elevation. Images were processed using Agisoft, a photogrammetry software. The resulting digital elevation model has a resolution of less than 1 mm (Figure 2). In order to compare hyporheic exchange with and without the influence of jams, the jams were removed and the image capture process was repeated.

2.2. Numerical Modeling

Surface water flow was represented using the two-dimensional shallow water equations:

$$\frac{\partial h}{\partial t} + \nabla \cdot \left(\overline{v} d_o\right) + d_o \Gamma_o = 0 \quad (1)$$

$$\frac{\partial \overline{v}}{\partial t} + \overline{v} \cdot \nabla\left(\overline{v}\right) + g \nabla d_o = g\left(\boldsymbol{S_o} - \boldsymbol{S_f}\right) \quad (2)$$

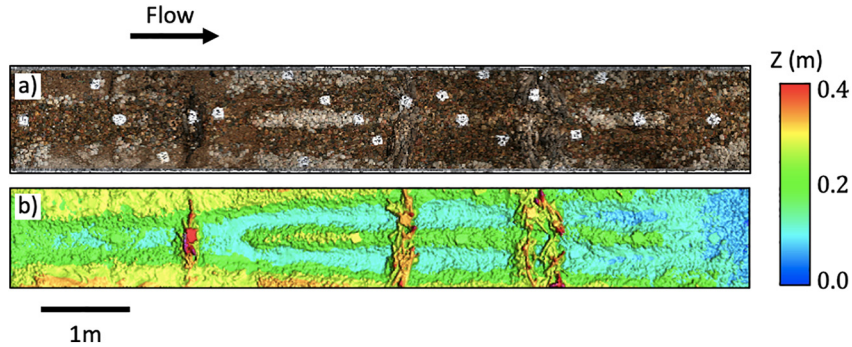

Figure 2. (a) Aerial image of flume structure. (b) Digital elevation model. White dots present in (a) are reference locations used in the photogrammetry processing.

where h is the water surface elevation in m (referenced to a fixed datum), d_o is the depth of flow in m (h minus the elevation of the sediment-water interface), $\overline{v}$ is the vertically averaged flow velocity in m/s, Γ_o is the exchange rate between the surface and subsurface domains in 1/s, g is the acceleration due to gravity in m/s^2, and $\boldsymbol{S_o}$ and $\boldsymbol{S_f}$ are dimensionless bed and friction slopes, respectively. Since the shallow water equations are depth-averaged, the gradient operators in Equations 1 and 2 are two-dimensional and operate in the x- and y-directions. $\boldsymbol{S_f}$ was calculated from the Manning equation as a function of flow velocities in the x- and y-directions, the depth of flow, and Manning's roughness coefficient. The roughness coefficient used for surface flow was 0.030, typical of gravel beds with no vegetation (Table 1) (Phillips & Tadayon, 2006). We tested a narrow range of n from 0.023 to 0.030, but the model results proved insensitive to these changes. $\boldsymbol{S_f}$ varied continuously throughout the surface channel and was greater in regions of shallower flows with larger velocities, such as near the jam-stream interface and downstream extent of the model. Through the interfacial exchange flux, Γ_o, Equations 1 and 2 were coupled to the three-dimensional variably saturated groundwater flow equation:

$$-\nabla \cdot \left(-K\, k_r \nabla\left(\psi + z\right)\right) + \Gamma_o = \frac{\partial}{\partial t}\left(\theta_s S_w\right) \tag{3}$$

where K is the hydraulic conductivity tensor in m/s, k_r is the relative permeability, ψ is pressure head in m, z is elevation head in m, θ_s is saturated water content (or porosity), and S_w is the degree of water saturation θ/θ_s, where θ is water content. The gradient operator for Equation 3 operates in the x-, y-, and z-directions. The relationship between water content and pressure head is controlled by the van Genuchten parameters (Table 1), which were chosen to be representative of sandy sediments (Zhu & Mohanty, 2002).

In Equations 1–3, water is assumed to be incompressible with uniform density. Equations 1 and 2 ignore vertical velocity structure that exists in recirculation zones and may, therefore, misrepresent the hydraulic head conditions immediately downstream of jam structures. However, any inaccuracies would be local and limited to the recirculation zones. The two-dimensional shallow water equations and three-dimensional variably saturated groundwater flow equation are suitable for our primary goal of resolving the overall, multiscale structure of hyporheic flow resulting from jams and branching channels. The shallow water equations have been used to simulate stream-groundwater interactions for a wide variety of complex, multidimensional flows, including cases where stream flow is fully turbulent (Chow et al., 2019; Heniche et al., 2000; Leclerc et al., 1990; Wang et al., 2002). Chow et al. (2019) showed that Equations 1–3 adequately characterize hyporheic exchange in a turbulent river so long as the model bathymetry resolves local-scale bedforms that drive hyporheic exchange (Chow et al., 2019). Other studies have shown that using Reynolds-averaged Navier-Stokes equations with a turbulence closure scheme can improve the representation of local hyporheic exchange processes in wakes and recirculation zones (Janssen et al., 2012; Zhou &

Table 1
Model Parameters and Values

Variable	Definition	Value	Units
S_w	Residual saturation	0.053	-
N	Manning's coefficient	0.030	s/m$^{1/3}$
θ_s	Porosity (sediment)	0.30	-
	van Genuchten alpha	3.548	1/m
	van Genuchten gamma	3.162	-
K_{shallow}	Hydraulic conductivity (upper layer)	2.5×10^{-2}	m/s
K_{deep}	Hydraulic conductivity (lower layer)	8.9×10^{-4}	m/s
K_{jam}	Hydraulic conductivity (jams)	1.0	m/s
θ_s	Porosity (jams)	0.70	-

Endreny, 2013), but these numerical models require more computational resources, particularly for flows with a free surface, and are often applied over small scales in practice.

The base and sides of the model were defined as no-flow boundaries to represent the bottom and sides of the flume environment. At the upstream boundary of the flume domain, a specified inflow flux was assigned to simulate the stepped spillway. At the downstream outlet, a critical depth boundary condition was established to match flume observations. The model was initialized with an impermeable bed and run until surface water flow approached steady state. These results were used as initial conditions for a second transient simulation with a permeable bed in order to achieve steady conditions in both the surface and subsurface.

Simulations were run using the control-volume finite element method in HydroGeoSphere (Huyakorn et al., 1986; Panday et al., 1993; Therrien, 1992; Therrien & Sudicky, 1996). The surface of the domain was discretized with an unstructured, triangular mesh with maximum element length of 2.0 cm. While the minimum element size is coarser than the resolution of the digital elevation model, a finer mesh would have been inconsistent with the concept of a porous continuum for the coarse sediments used in the flume. The subsurface was discretized using two porous media domains. The deeper porous media elements were assigned element heights of 0.028 m, while the three near-surface sediment layers were assigned element heights of 0.005 m. Jam structures were represented in the model as additional porous media domains that extended above the height of the surface water and acted as permeable dams. The decision to treat the jams as porous media was both precedented and practical. Field and numerical studies have previously considered jams as porous media and estimated their porosities (Spreitzer et al., 2020; van Gent, 1994; Xu & Liu, 2017). Treating flow through the jams as a free flow instead of a flow through porous media would have required full three-dimensional solutions to the Navier-Stokes equations. Our interest was not in understanding the velocity fields within the jams but their effect on hydraulic heads and hyporheic exchange, which should be well represented in the chosen model framework (Ventres-Pake et al., 2020; Xu & Liu, 2017). General model performance was checked by comparing a solute transport simulation with flume tracer experimental results (Supporting Information S1).

Particle tracking was used to visualize hyporheic flow paths in Tecplot and analyze hyporheic residence time distributions. Specifically, particles were released along the sediment-water interface from fully saturated model nodes with downward-directed fluid flux, and they were tracked while they remained in the sediment. In reach-scale residence time distributions, particles were released across the entire saturated sediment-water interface; in residence time distributions for individual jams, particles were only released from the pool upstream of each jam. Frequencies of particle residence times and path lengths were flux weighted. The total number of particles tracked across individual jams varied between 1,096 and 3,950, while the total number of particles across the reach varied between 16,352 and 31,575, depending on runs. We did not include particles with path lengths less than 0.01 m, the approximate length scale of individual sediment grains, in our residence time or particle path distributions.

We computed additional reach-scale hyporheic metrics to compare simulations with and without jam structures, including the average hyporheic exchange rate and the turnover length. The average hyporheic exchange rate (q_{swi}), in m/s, was computed by integrating the positive (upwelling) exchange fluxes across the bed and dividing by the wetted streambed area, A, in m^2. Positive exchange fluxes were used to only consider exchange that eventually resurfaces into the surface channel and exclude flow that downwells and exits through the subsurface outflow at the downstream extent of the simulation domain. The degree of hyporheic connectivity was calculated as the turnover length (L), or average distance water travels downstream before it enters the bed, in m (Harvey & Wagner, 2000; Newbold et al., 1983):

$$L = \frac{Q}{q_{\mathrm{swi}} A} L_f \tag{4}$$

where Q is stream discharge in m^3/s and L_f is the length of the flume in m. Turnover length is a useful metric for considering the potential impacts of hyporheic exchange on stream water quality, assuming chemical transformations predominantly occur within the streambed.

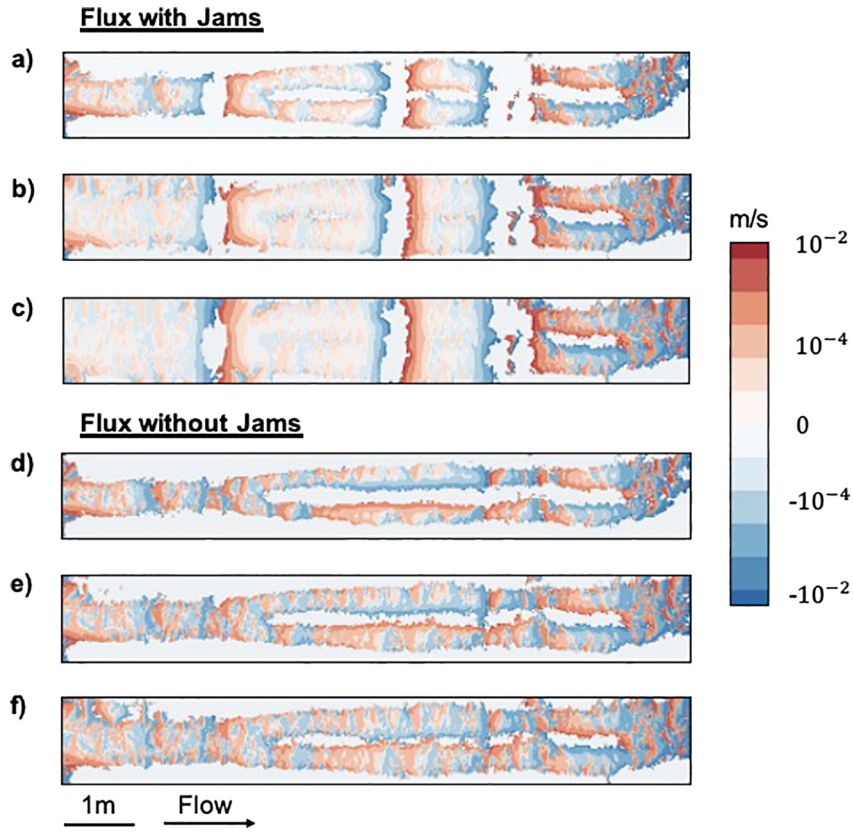

Figure 3. Hyporheic exchange flux maps across the wetted streambed for: (a) low-flow, (b) medium-flow, and (c) high-flow conditions for the simulations with jam structures, and (d) low-flow, (e) medium-flow, and (f) high-flow conditions for the simulations with no jam structures. Positive values indicate upwelling and negative values indicate downwelling.

3. Results

3.1. Effect of Jam Structures on Exchange Rates and Connectivity

Around jam structures, downwelling characteristically occurs in the upstream pools, and upwelling occurs in the downstream channels (Figures 3a–3c). Away from jam structures, exchange patterns are dominated by short flow paths on the length scale of irregularities in the planar bed (~3–10 cm). The average hyporheic exchange rate increases with streamflow from 1.3×10^{-3} m/s to 3.5×10^{-3} m/s for stream discharge rates of 1.4–8.5 L/s. This corresponds with observed increases in stream depth and head gradients along the sediment-water interface, particularly in the pools above the jams. For comparison, simulations without jams lack the larger-scale exchange patterns (Figures 3d–3f). The average exchange flux rate is far lower (2.1×10^{-4} m/s–2.9×10^{-4} m/s) and changes little with stream discharge, consistent with Zhang et al. (2021). The exchange rates in volumetric units are equivalent to 221%–285% of stream discharge with jams and 11%–58% of stream discharge without jams. Although we were not focused on net gains or losses from the stream, it is worth noting that the stream was generally losing both with and without jams. Net losses ranged from 1.0 to 1.2 L/s, depending on the stream discharge rate and presence or absence of jams.

Jams not only increase average exchange rates but also create more area for exchange by creating backwater effects, particularly under higher stream discharge rates. Under medium- and high-stream flow rates, the wetted streambed area increases by 37%–38%. At low-flow rates, the wetted streambed area only increases 9% with jams.

Turnover length substantially decreases in the presence of jam structures due to both changes in the area available for exchange and the flux across the bed. In the presence of jams, the turnover lengths for the low, medium, and high stream flows are 1.83, 1.85, and 1.97 m, respectively. Without jams, the lengths are

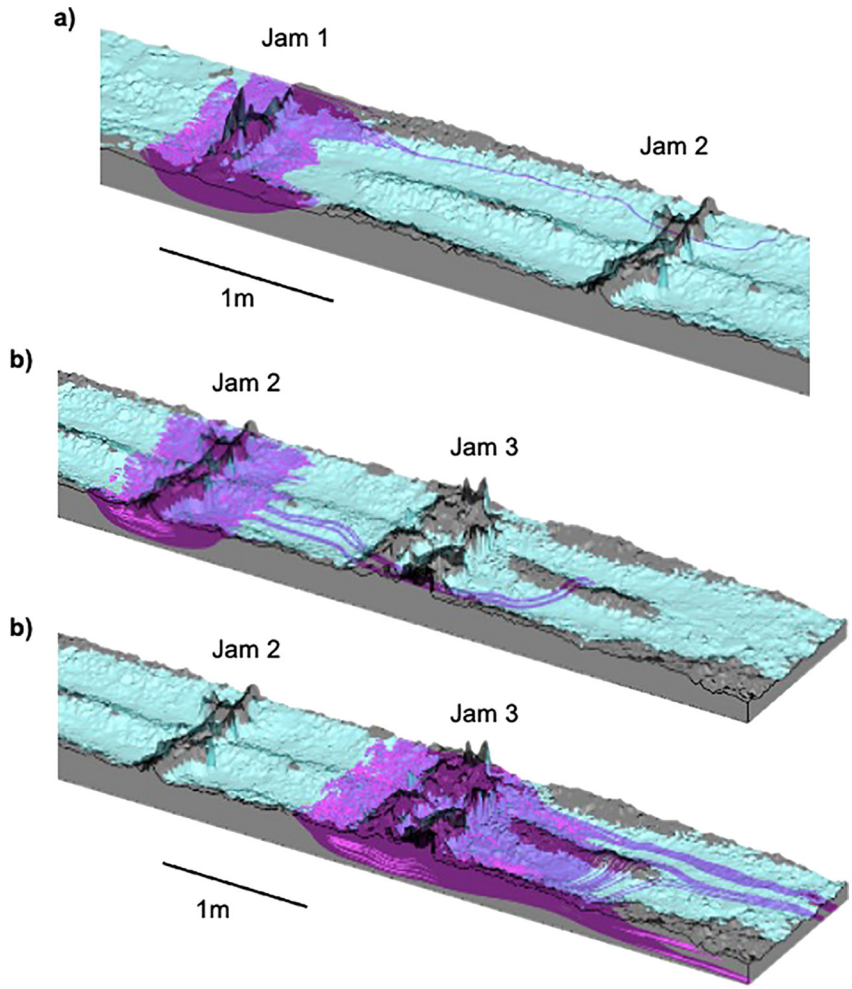

Figure 4. Flow paths (purple) across (a) Jam 1, (b) Jam 2, and (c) Jam 3 for medium discharge. Most downwelling flow upstream of Jam 1 upwells immediately downstream of the structure. Although the hyporheic flow paths associated with Jam 2 and Jam 3 are largely independent of each other, some flow paths that originate at Jam 2 extend downstream and return to the stream below Jam 3 in the gravel bar.

8.62, 24.1, and 45.4 m, respectively. Only 9%–38% of the differences in turnover lengths with and without jams are due to the increase in wetted streambed area (A in Equation 4), while the remainder is due to the increase in exchange flux (q_{swi} in Equation 4).

3.2. Complexities in Hyporheic Flow Paths and Residence Times

Hyporheic flow paths around jams vary depending on their position within single or multiple channel threads and also across stream flow rates. In the single channel around Jam 1, water downwells under the jam structure and upwells immediately downstream of the jam with only little interaction with the channel banks (Figure 4a). However, in the multithreaded channel system, hyporheic flow paths span Jams 2 and 3 and interact with the central gravel bar (Figures 4b and 4c). Some of the downwelling flow that originates in the pool upstream of Jam 2 travels through the hyporheic zone and resurfaces downstream of Jam 3 in the gravel bar separating the channels. Similarly, some of the hyporheic flow originating in the pool upstream of Jam 3 travels under the jam structure and moves laterally into the stream banks. A portion of this flow exits the subsurface at the downstream extent of the flume and would have presumably resurfaced even farther downstream if not for the finite flume length. In addition to the interactions between jams and the multithreaded channel, it also appears that jams interact with one another to affect longer hyporheic flow paths. For example, Jams 2 and 3 drive upwelling of flows that originated above Jams 1 and 2, thereby

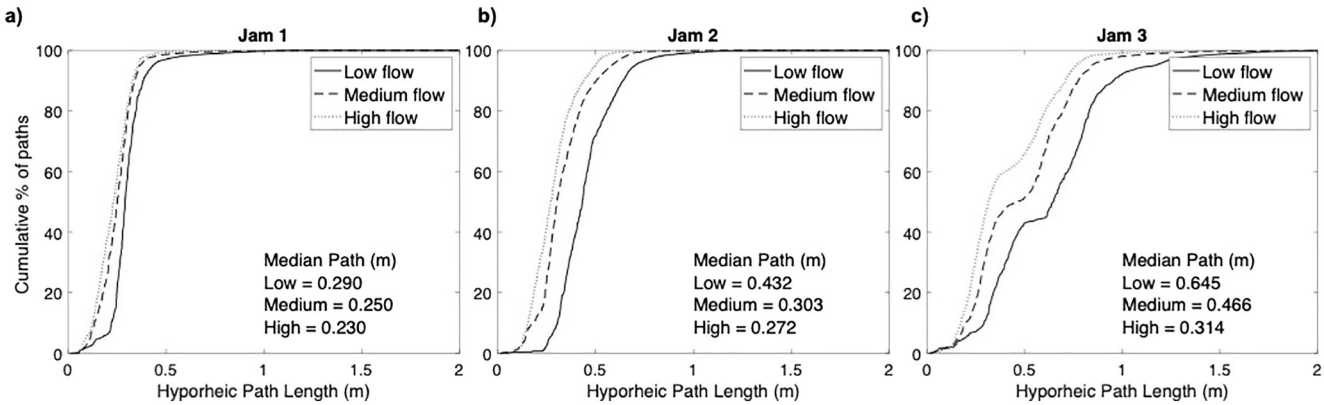

Figure 5. Flux-weighted distributions of hyporheic flow path lengths across (a) Jam 1, (b) Jam 2, and (c) Jam 3. Jam 1 is farthest upstream within a single channel. Jams 2 and 3 are farther downstream in multi-threaded channel sections.

shortening their path lengths. The deepest flow paths directly under the jam structures are constrained by the bottom of the model for all three flow conditions, highlighting that sediment thickness is an important control on the depth of hyporheic flow.

Hyporheic path length distributions (Figure 5) differ substantially in shape as jam volume and complexity increase from Jam 1 to Jam 3. The largest and most complex jam (Jam 3) clearly shows multiple modes of path lengths, indicating the diverse scales of exchange in the presence of both large jam volume and a branched channel. The shortest path lengths at Jam 3 (<0.5 m) initiate in the pool immediately upstream and terminate in the jam itself and immediately downstream. Meanwhile, longer path lengths (>0.5 m) terminate in the channel farther downstream, including areas along the gravel bar between the channels. Jam 3 also has the broadest distribution of path lengths (Figure 5c). For example, the difference between the 25th and 90th percentile path lengths at the low-flow condition is 0.59 m for Jam 3, compared to 0.13 and 0.29 m for Jams 1 and 2, respectively. These distributions shift slightly with stream discharge: as streamflow increases, flow paths become shorter (Figures 5 and 6).

For a given stream discharge, median path length increases with jam complexity and volume from Jam 1 to Jam 3 (Figures 5 and 6). Larger jams have longer median flow path lengths (50th percentile) and longer extreme flow path lengths (90th percentile) (Figure 6). This suggests that larger jams have a particular capacity to drive long hyporheic flow that spans multiple channel features. Interestingly, the longest lengths appear to be less sensitive to stream flow rate than the median path lengths (compare the range of path

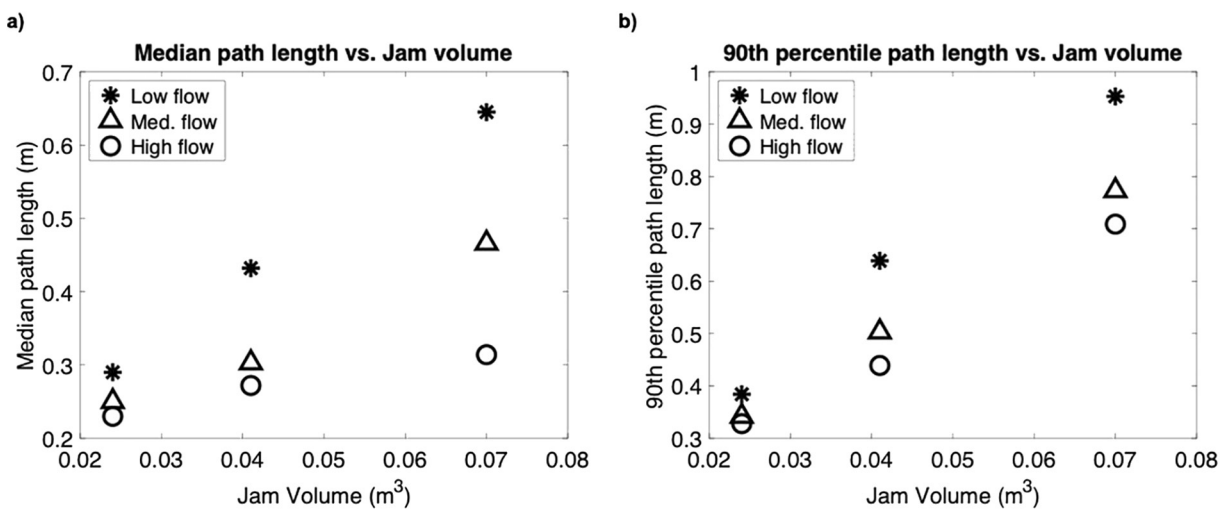

Figure 6. Hyporheic path length increases with jam volume, both for (a) the median path length and (b) the longer flow paths (90th percentile).

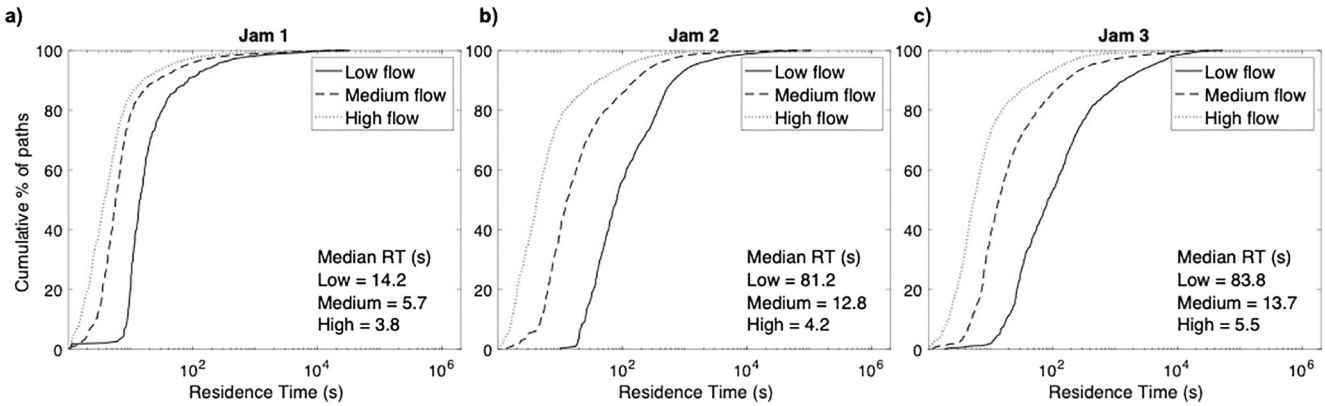

Figure 7. Flux-weighted distributions of hyporheic residence times across (a) Jam 1, (b) Jam 2, and (c) Jam 3. Jam 1 is upstream, and Jam 3 is downstream (locations are shown in Figure 1). Note the semilogarithmic scale, unlike Figure 5.

lengths across stream flow conditions for the largest jam volume of 0.07 m^3 in Figures 6a and 6b). In other words, the longer flows are relatively robust across a range of stream flow conditions. These complex trends show the nonlinear interactions between stream flow rate and the factors that drive hyporheic exchange, which range from hydraulic head gradients to wetted channel extent.

Hyporheic residence times beneath individual jams generally decrease with increasing stream flow rate (Figure 7). Jams 2 and 3, which are larger and interact with multiple channel threads, have increased ranges of residence times associated with distinct flow path lengths. The faster residence times are associated with shallower flow paths that resurface downstream in the channel closer to the jam structure, while the longer residence times are associated with deeper, slower flow paths that migrate farther downstream including through the gravel bar separating the channels. The orders-of-magnitude range and relatively smooth distribution in residence times at Jam 3 in particular (Figure 7c) can be explained by the combination of multimodal flow path lengths (Figure 5c) and high variability of seepage rates along those flow paths.

In model runs without jams, reach-scale hyporheic flow paths are much shorter (Figure 8), and median residence times are generally longer than model runs with jams, especially for greater stream-flow conditions (Figure 9). In other words, hyporheic flows without jams are short and sluggish. Overall, this is consistent

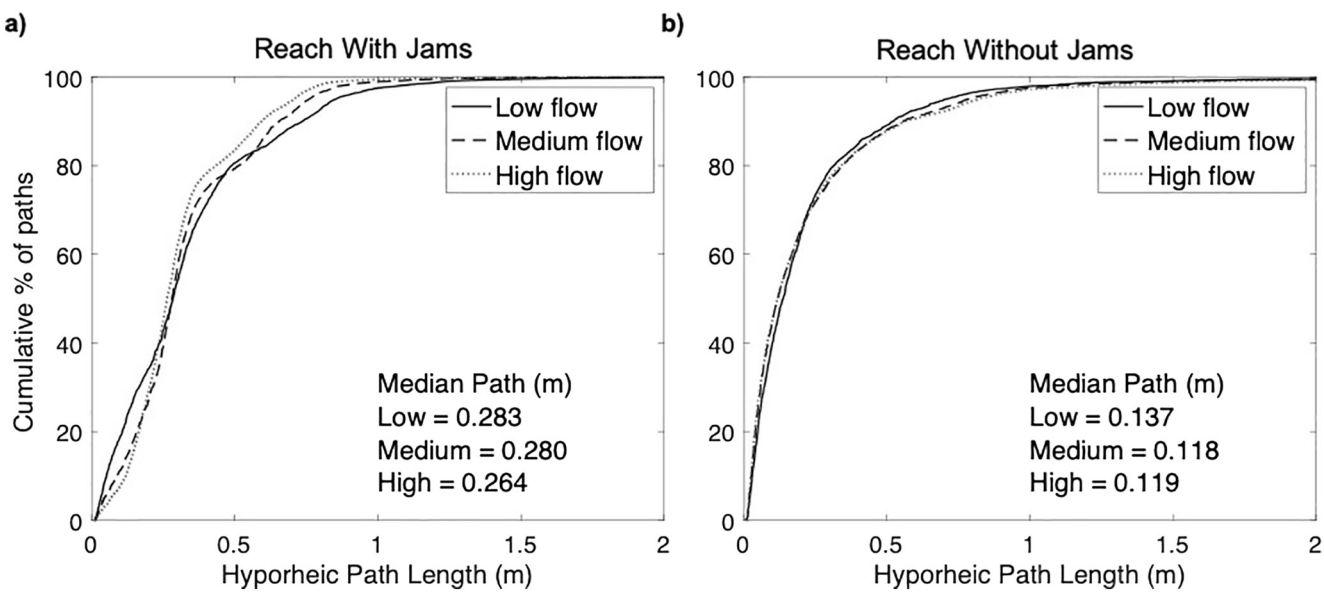

Figure 8. Reach-scale hyporheic path length distributions for model simulations (a) with jams and (b) without jams.

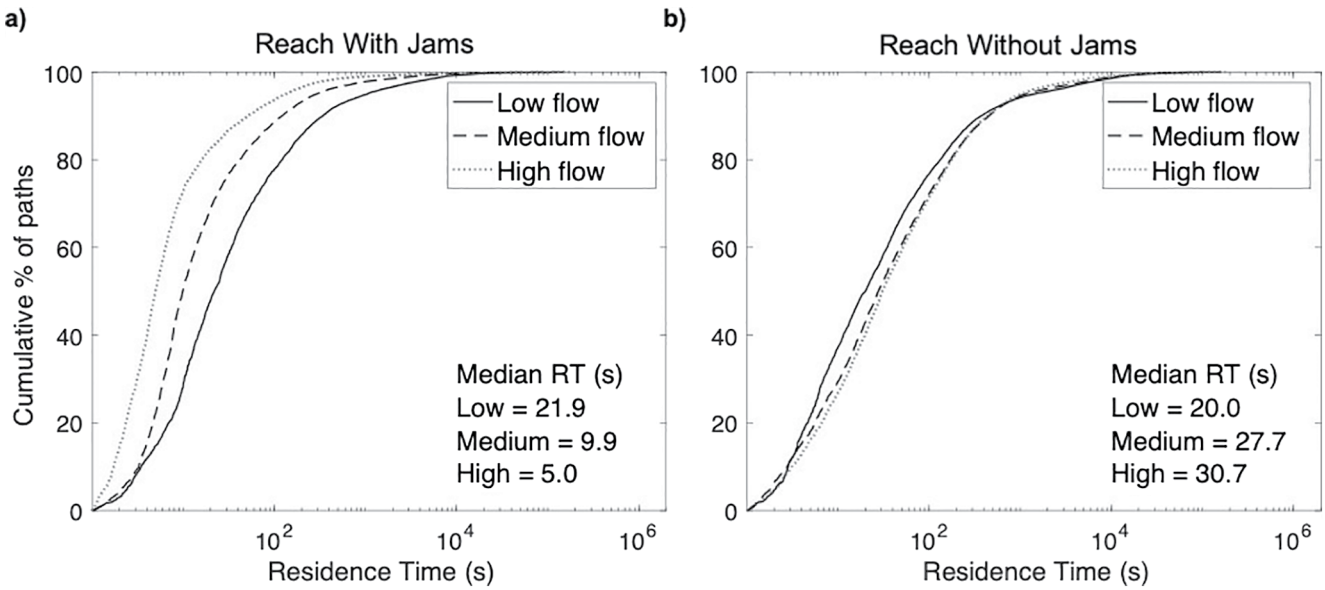

Figure 9. Reach-scale hyporheic residence time distributions for model simulations (a) with jams and (b) without jams.

with the reduction in exchange fluxes in the absence of jams. The net effect is that the hyporheic zone is more disconnected and acts as more of an immobile zone due to low bed exchange rates.

4. Discussion

These simulations reveal that: (a) jam structures drive larger hyporheic exchange rates, potentially impacting water quality, (b) the combination of large jams and multithreaded channels creates opportunities for hyporheic flow paths that span a wide range of length and time scales.

4.1. Jam Structures Drive Hyporheic Flow and Chemical Reaction Potential in the Hyporheic Zone

Our simulations suggest that gravel streams with log jams have much greater hyporheic exchange rates, especially under high stream flow, resulting in more effective turnover. This turnover is due to both the greater wetted streambed area created by backwater effects and the faster fluxes near jams, but particularly the latter. In the flume environment, wetted area only increases by 9%–38% when jams are added (depending on stream flow rate), while exchange rates increase by one or more orders of magnitude. Most hyporheic modeling studies do not separate these effects because they are either two-dimensional (Cardenas & Wilson, 2007; Salehin et al., 2004; Sawyer et al., 2011) or three-dimensional with a fixed, predefined wetted area (Cardenas et al., 2004; Doughty et al., 2020; but see Tonina & Buffington, 2007 and Trauth et al., 2015 for exceptions). While this study suggests that hyporheic fluxes are more responsive than wetted area to changes in jam structure or stream discharge, the behavior may differ in the field, where floodplains can be extensive and thick vegetation can divert flow from the main channel (Majerova et al., 2015; Nyssen et al., 2011). Majerova et al. (2015) found that less than two years after the establishment of a beaver dam in Curtis Creek in Northern Utah, the total water surface area had more than doubled. Observations of a beaver dam built on top of a log jam during the course of our field measurements at Little Beaver Creek indicate similar increases in backwater storage of water, fine sediment, and particulate organic matter.

Gains in hyporheic connectivity due to jams may have substantial effects on stream water quality. Turnover length and hyporheic residence time together control stream water chemistry, as represented by the reaction significance factor per kilometer, RSF (Harvey & Fuller, 1998):

$$\mathrm{RSF} = \frac{\lambda t_{hz} 1000}{L} \quad (5)$$

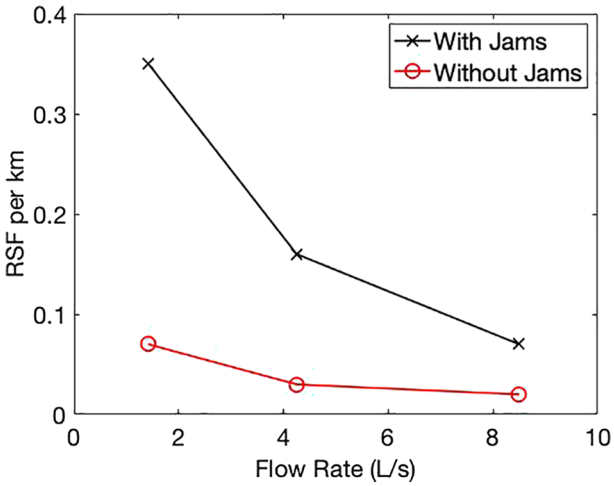

Figure 10. Reaction significance factor per km as a function of stream flow rate for simulations with and without jams. In this case, the reaction of interest is denitrification.

where λ is the reaction rate (1/s), t_{hz} is the hyporheic residence time (s), and L is the turnover length (m). The reaction significance factor relates the amount of time water spends in the hyporheic zone as it flows downstream with the time required for chemical transformations. Greater values indicate more complete chemical processing over a given reach length (Harvey & Fuller, 1998). The length scale of one kilometer was used in this analysis to consider potential transformations in a longer system than the flume. In our model trials, simulations with jams had shorter residence times, allowing for less complete chemical processing during a given excursion through the hyporheic zone, but much greater turnover along a reach, allowing for cumulatively more impact on stream water quality, especially at low to medium stream flow rates. For example, assuming a typical reaction rate constant for denitrification in the subsurface of $3 \times 10^{-5}\,s^{-1}$ ($0.1\,h^{-1}$) (Harvey et al., 2013), the reaction significance factor per kilometer would range from 0.02 to 0.07 in our simulations without jams to 0.07–0.35 in our simulations with jams (Figure 10). The effect of jams on reactions such as denitrification (Harvey et al., 2013; Zarnetske et al., 2011) and manganese oxidation (Harvey & Fuller, 1998) is substantial, particularly at low-flow conditions, which is generally when hydrologic retention (t_{hz}/L in Equation 5) is expected to be greatest in streams (Harvey et al., 1996; Morrice et al., 1997). Hydrologic retention has also been shown to scale with frictional resistance (Harvey et al., 2003), which is enhanced by jams and their associated morphologic changes like channel braiding, pools, and riffles (Trauth et al., 2013). The connection between frictional resistance and hydrologic retention may offer a path forward for predicting the effects of jams on hyporheic processes, but this idea would need to be tested with field experiments.

It is unclear how hyporheic metrics from these flume-scale experiments upscale to the field. In flume experiments and models, Froude numbers were less than 0.1, similar to the field site that inspired the flume experiments, Little Beaver Creek. Sediment and jam permeabilities were likely greater in the flume than many field settings, at least in a scaled sense. However, field-scale estimates of jam permeabilities are generally unknown and are an interesting area for future research. The net result is that specific magnitudes of bed exchange fluxes, hyporheic path lengths, and hyporheic residence times at the field scale cannot be determined from flume-scale experiments, but general qualities (for example, the existence of multiple modes of exchange lengths near more complex jams and the substantial increase in exchange rates and reaction significance with jams) should be consistent across flume to field scales.

4.2. Multiple Channel Threads and Big Jams Increase Hyporheic Interactions

This study shows that big jams with multiple channel threads encourage multidimensional hyporheic interaction, even for the relatively simple, two-channel system examined here. The flume and model geometry underrepresents the complexities present in anabranching stream systems with jams observed in nature. As jam structures accumulate in a stream channel, upstream pooling increases, driving surface and hyporheic flow paths through the floodplain and aggraded gravel bars, leading to channel avulsion and heightened complexity of the stream system (Abbe & Montgomery, 1996; Mosley, 1981; Sear et al., 2010). Therefore, evolution in channel and jam complexity results in the activation of the floodplain and other portions of the hyporheic system that would otherwise be dormant (Doughty et al., 2020; Gooseff et al., 2006; Morrice et al., 1997; Wondzell et al., 2009). Changes in inundation area have been shown to have a profound influence on hyporheic connectivity at field scales on the order of tens of square kilometers (Helton et al., 2014). Future research needs to consider the more complex formation of numerous side channels and flow paths in and around log jams. Models that incorporate greater morphologic complexity and changes in inundation area should reveal even greater influence of jams on multidimensional hyporheic flows.

Comparing the second and third jams in the flume, it also appears that larger jams are particularly effective at initiating longer hyporheic flow paths and can promote multiple dominant exchange length scales and residence times. In the flume, these longer, deeper flow paths might be constrained by the base of the

sediment box. The extent of these flows in natural streams could depend strongly on the depth of alluvial cover (Tonina & Buffington, 2009), which is in turn influenced by the presence of large wood, since jams store sediments (Massong & Montgomery, 2000; Montgomery et al., 2003). The interacting effect of jams, sediment storage, and longer, deeper hyporheic exchange flows cannot be tested in these experiments but is an area for future research.

It is important to ask what is more important for hyporheic connectivity and solute transport—a smaller number of large jams or many smaller jams. Mutz et al. (2007) found that a fairly even distribution of many small wood pieces across a flume channel increased the flux, volume, and depth of the active hyporheic zone. They did not test the effects of uneven jam-like distributions. Dudunake et al. (2020) observed a similar increase in exchange around many relatively evenly spaced boulders in a flume. The structure of wood pieces and their orientation and grouping are likely to have a wide range of effects on wetted channel area and pooling upstream of jams that we are unable to test with our jam representation in the current model framework. Interestingly, the largest jam structure (Jam 3) had strikingly multimodal path lengths and a wide distribution of residence times. Larger jams have the ability to generate increased upstream pooling and alter stream energy gradients, as detailed by Faustini and Jones (2003), which may lead to particularly unique hyporheic exchange characteristics. This may help explain anomalous, bimodal solute breakthrough behavior that was observed in a field tracer experiment downstream of a large jam (Doughty et al., 2020). Successful application of stream management plans utilizing log jams is dependent upon understanding the hyporheic effects of different large wood distributions (ranging from more dispersed distributions to many smaller, successional jam structures to fewer, larger jams).

Log jams were prevalent features of pre-settlement rivers, but the practice of channel clearing has since reduced log jams (Wohl, 2019). This study, along with several others (e.g., Briggs et al., 2013; Krause et al., 2014; Sawyer & Cardenas, 2012), suggests that hyporheic flows in post-settlement rivers have fundamentally changed in terms of path lengths, residence times, and flux patterns. However, these studies also suggest that river-groundwater connectivity, and possibly chemical processing and nutrient retention, can be restored through the management of wood loads or in-stream obstructions, for example by maintaining natural in-stream wood loads or preserving conditions for beaver habitat survival or reestablishment (Hester & Gooseff, 2010; Lautz et al., 2019).

5. Conclusions

The presence of log jam structures increases channel wetted area and bed hyporheic exchange flux, particularly the latter, driving longer subsurface flow paths that connect multiple jam structures. Jams facilitate more opportunities for solute retention and processing in the hyporheic zone, especially at lower flow rates, when hydrologic retention peaks. This study further highlights the influence that larger log jams in combination with multiple channel branches have on hyporheic systems, namely increased ranges of hyporheic length and time scales. The resulting effects of these jam-induced hyporheic patterns on chemical processes, measured by the reaction significance factor, emphasizes the value of log jams on overall stream function. Areas for further research include determining how jam frequency and the properties of individual jams (permeability and porosity) influence the coevolution of channel morphology and hyporheic flow in forested streams.

Acknowledgments
This research was supported by the National Science Foundation (EAR-1819086) and the Geological Society of America through a student research grant to K. Wilhelmsen. The authors thank the Associate Editor and two anonymous reviewers for comments that improved the manuscript. We also thank Michael Durand and Joachim Moortgat for discussion and insights on the numerical simulations and research approach.

Data Availability Statement

An example of a model input file is available in the appendix of Wilhelmsen (2021).

References

Abbe, T. B., & Montgomery, D. R. (1996). Large woody debris jams, channel hydraulics, and habitat formation in large rivers. *Regulated Rivers: Research & Management*, *12*, 201–221. https://doi.org/10.1002/(SICI)1099-1646(199603)12:2/3<201::AID-RRR390>3.0.CO;2-A

Ader, E., Wohl, E., McFadden, S., & Singha, K. (2021). Logjams as a driver of transient storage in a mountain stream. *Earth Surface Processes and Landforms*, *46*(3), 701–711. https://doi.org/10.1002/esp.5057

Arrigoni, A. S., Poole, G. C., Mertes, L. A. K., O'Daniel, S. J., Woessner, W. W., & Thomas, S. A. (2008). Buffered, lagged, or cooled? Disentangling hyporheic influences on temperature cycles in stream channels. *Water Resources Research*, *44*(9). https://doi.org/10.1029/2007WR006480

Beckman, N. D., & Wohl, E. (2014). Carbon storage in mountainous headwater streams: The role of old-growth forest and logjams. *Water Resources Research*, *50*(3), 2376–2393. https://doi.org/10.1002/2013WR014167
Briggs, M. A., Lautz, L. K., Hare, D. K., & Gonzalez-Pinzon, R. (2013). Relating hyporheic fluxes, residence times, and redox-sensitive biogeochemical processes upstream of beaver dams. *Freshwater Science*, *32*(2), 622–641. https://doi.org/10.1899/12-110.1
Buffington, J. M., & Tonina, D. (2009). Hyporheic Exchange in Mountain Rivers II: Effects of Channel Morphology on Mechanics, Scales, and Rates of Exchange. *Geography Compass*, *3*(3), 1038–1062. https://doi.org/10.1111/j.1749-8198.2009.00225.x
Cardenas, M. B., & Wilson, J. L. (2007). Dunes, turbulent eddies, and interfacial exchange with permeable sediments: Dunes, eddies, and interfacial exchange. *Water Resources Research*, *43*(8). https://doi.org/10.1029/2006wr005787
Cardenas, M. B., Wilson, J. L., & Zlotnik, V. A. (2004). Impact of heterogeneity, bed forms, and stream curvature on subchannel hyporheic exchange: Modeling study of hyporheic exchange. *Water Resources Research*, *40*(8). https://doi.org/10.1029/2004WR003008
Chow, R., Wu, H., Bennett, J. P., Dugge, J., Wöhling, T., & Nowak, W. (2019). Sensitivity of simulated hyporheic exchange to river bathymetry: The Steinlach river test site. *Groundwater*, *57*(3), 378–391. https://doi.org/10.1111/gwat.12816
Collins, B. D., Montgomery, D. R., Fetherston, K. L., & Abbe, T. B. (2012). The floodplain large-wood cycle hypothesis: A mechanism for the physical and biotic structuring of temperate forested alluvial valleys in the North Pacific coastal ecoregion. *Geomorphology*, *139–140*, 460–470. https://doi.org/10.1016/j.geomorph.2011.11.011
Crenshaw, C. L., Valett, H. M., & Webster, J. R. (2002). Effects of augmentation of coarse particulate organic matter on metabolism and nutrient retention in hyporheic sediments. *Freshwater Biology*, *47*(10), 1820–1831. https://doi.org/10.1046/j.1365-2427.2002.00928.x
Curran, J. H., & Wohl, E. E. (2003). Large woody debris and flow resistance in step-pool channels, Cascade Range, Washington. *Geomorphology*, *51*(1), 141–157. https://doi.org/10.1016/S0169-555X(02)00333-1
Dolzyk, K., & Chmielewska, I. (2014). Predicting the Coefficient of Permeability of Non-Plastic Soils. *Soil Mechanics and Foundation Engineering*, *51*(5), 213–218. https://doi.org/10.1007/s11204-014-9279-3
Doughty, M., Sawyer, A. H., Wohl, E., & Singha, K. (2020). Mapping increases in hyporheic exchange from channel-spanning logjams. *Journal of Hydrology*, *587*, 124931. https://doi.org/10.1016/j.jhydrol.2020.124931
Dudunake, T., Tonina, D., Reeder, W. J., & Monsalve, A. (2020). Local and reach-scale hyporheic flow response from Boulder-induced geomorphic changes. *Water Resources Research*, *56*(10), e2020WR027719. https://doi.org/10.1029/2020WR027719
Endreny, T., Lautz, L., & Siegel, D. I. (2011). Hyporheic flow path response to hydraulic jumps at river steps: Flume and hydrodynamic models. *Water Resources Research*, *47*(2). https://doi.org/10.1029/2009WR008631
Evans, E. C., & Petts, G. E. (1997). Hyporheic temperature patterns within riffles. *Hydrological Sciences Journal*, *42*(2), 199–213. https://doi.org/10.1080/02626669709492020
Faustini, J. M., & Jones, J. A. (2003). Influence of large woody debris on channel morphology and dynamics in steep, boulder-rich mountain streams, western Cascades, Oregon. *Geomorphology*, *51*(1), 187–205. https://doi.org/10.1016/S0169-555X(02)00336-7
Freeze, R. A., & Cherry, J. A. (1979). *Groundwater*. Prentice-Hall.
Gandy, C. J., Smith, J. W. N., & Jarvis, A. P. (2007). Attenuation of mining-derived pollutants in the hyporheic zone: A review. *The Science of the Total Environment*, *373*(2), 435–446. https://doi.org/10.1016/j.scitotenv.2006.11.004
Gooseff, M. N., Anderson, J. K., Wondzell, S. M., LaNier, J., & Haggerty, R. (2006). A modelling study of hyporheic exchange pattern and the sequence, size, and spacing of stream bedforms in mountain stream networks, Oregon, USA. *Hydrological Processes*, *20*(11), 2443–2457. https://doi.org/10.1002/hyp.6349
Harvey, J. W., Böhlke, J. K., Voytek, M. A., Scott, D., & Tobias, C. R. (2013). Hyporheic zone denitrification: Controls on effective reaction depth and contribution to whole-stream mass balance. *Water Resources Research*, *49*, 6298–6316. https://doi.org/10.1002/wrcr.20492
Harvey, J. W., Conklin, M. H., & Koelsch, R. S. (2003). Predicting changes in hydrologic retention in an evolving semi-arid alluvial stream. *Advances in Water Resources*, *26*(9), 939–950. https://doi.org/10.1016/S0309-1708(03)00085-X
Harvey, J. W., & Fuller, C. C. (1998). Effect of enhanced manganese oxidation in the hyporheic zone on basin-scale geochemical mass balance. *Water Resources Research*, *34*(4), 623–636. https://doi.org/10.1029/97WR03606
Harvey, J. W., & Wagner, B. J. (2000). Quantifying hydrologic interactions between streams and their subsurface hyporheic zones. *Streams and ground waters* (pp. 3–44). Elsevier. https://doi.org/10.1016/B978-012389845-6/50002-8
Harvey, J. W., Wagner, B. J., & Bencala, K. E. (1996). Evaluating the reliability of the stream tracer approach to characterize stream-subsurface water exchange. *Water Resources Research*, *32*(8), 2441–2451. https://doi.org/10.1029/96WR01268
Helton, A. M., Poole, G. C., Payn, R. A., Izurieta, C., & Stanford, J. A. (2014). Relative influences of the river channel, floodplain surface, and alluvial aquifer on simulated hydrologic residence time in a montane river floodplain. *Geomorphology*, *205*, 17–26. https://doi.org/10.1016/j.geomorph.2012.01.004
Heniche, M., Secretan, Y., Boudreau, P., & Leclerc, M. (2000). A two-dimensional finite element drying-wetting shallow water model for rivers and estuaries. *Advances in Water Resources*, *23*(4), 359372. https://doi.org/10.1016/s0309-1708(99)00031-7
Hester, E. T., & Gooseff, M. N. (2010). Moving beyond the banks: Hyporheic restoration is fundamental to restoring ecological services and functions of streams. *Environmental Science & Technology*, *44*(5), 1521–1525. https://doi.org/10.1021/es902988n
Huyakorn, P. S., Springer, E. P., Guvanasen, V., & Wadsworth, T. D. (1986). A three-dimensional finite-element model for simulating water flow in variably saturated porous media. *Water Resources Research*, *22*(13), 1790–1808. https://doi.org/10.1029/WR022i013p01790
Janssen, F., Cardenas, M. B., Sawyer, A. H., Dammrich, T., Krietsch, J., & de Beer, D. (2012). A comparative experimental and multiphysics computational fluid dynamics study of coupled surface–subsurface flow in bed forms. *Water Resources Research*, *48*, W08514. https://doi.org/10.1029/2012WR011982
Krause, S., Hannah, D. M., Fleckenstein, J. H., Heppell, C. M., Kaeser, D., Pickup, R., et al. (2011). Inter-disciplinary perspectives on processes in the hyporheic zone. *Ecohydrology*, *4*(4), 481–499. https://doi.org/10.1002/eco.176
Krause, S., Klaar, M., Hannah, D., Mant, J., Bridgeman, J., Trimmer, M., & Manning-Jones, S. (2014). The potential of large woody debris to alter biogeochemical processes and ecosystem services in lowland rivers. *WIREs Water*, *1*, 263–275. https://doi.org/10.1002/wat2.1019
Lautz, L., Kelleher, C., Vidon, P., Coffman, J. M., Riginos, C., & Copeland, H. (2019). Restoring stream ecosystem function with beaver dam analogues: Let's not make the same mistake twice. *Hydrological Processes*, *33*, 174–177. https://doi.org/10.1002/hyp.13333
Lautz, L. K., Siegel, D. I., & Bauer, R. L. (2006). Impact of debris dams on hyporheic interaction along a semi-arid stream. *Hydrological Processes*, *20*(1), 183–196. https://doi.org/10.1002/hyp.5910
Leclerc, M., Bellemare, J.-F., Dumas, G., & Dhatt, G. (1990). A finite element model of estuarian and river flows with moving boundaries. *Advances in Water Resources*, *13*(4), 158168. https://doi.org/10.1016/0309-1708(90)90039-7
Livers, B., & Wohl, E. (2016). Sources and interpretation of channel complexity in forested subalpine streams of the Southern Rocky Mountains: Channel complexity in forested streams. *Water Resources Research*, *52*(5), 3910–3929. https://doi.org/10.1002/2015WR018306

Majerova, M., Neilson, B. T., Schmadel, N. M., Wheaton, J. M., & Snow, C. J. (2015). Impacts of beaver dams on hydrologic and temperature regimes in a mountain stream. *Hydrology and Earth System Sciences*, *19*(8), 3541–3556. https://doi.org/10.5194/hess-19-3541-2015

Massong, T. M., & Montgomery, D. R. (2000). Influence of sediment supply, lithology, and wood debris on the distribution of bedrock and alluvial channels. *The Geological Society of America Bulletin*, *112*(4), 591–599. https://doi.org/10.1130/0016-7606(2000)112<591:iossla>2.0.co;2

Montgomery, D. R., & Buffington, J. M. (1997). Channel-reach morphology in mountain drainage basins. *The Geological Society of America Bulletin*, *109*(5), 596–611. https://doi.org/10.1130/0016-7606(1997)109<0596:crmimd>2.3.co;2

Montgomery, D. R., Massong, T. M., & Hawley, S. C. S. (2003). Influence of debris flows and log jams on the location of pools and alluvial channel reaches, Oregon Coast Range. *GSA Bulletin*, *115*(1), 78–88. https://doi.org/10.1130/0016-7606(2003)115<0078:IODFAL>2.0.CO;2

Morrice, J. A., Valett, H. M., Dahm, C. N., & Campana, M. E. (1997). Alluvial Characteristics, groundwater-surface water exchange and hydrological retention in headwater streams. *Hydrological Processes*, *11*, 253–267. https://doi.org/10.1002/(sici)1099-1085(19970315)11:3<253::aid-hyp439>3.0.co;2-j

Mosley, M. P. (1981). The influence of organic debris on channel morphology and bedload transport in a New Zealand forest stream. *Earth Surface Processes and Landforms*, *6*(6), 571–579. https://doi.org/10.1002/esp.3290060606

Mutz, M., Kalbus, E., & Meinecke, S. (2007). Effect of instream wood on vertical water flux in low-energy sand bed flume experiments. *Water Resources Research*, *43*(10). https://doi.org/10.1029/2006WR005676

Newbold, J. D., Elwood, J. W., O'Neill, R. V., & Sheldon, A. L. (1983). Phosphorus dynamics in a woodland stream ecosystem: A study of nutrient spiralling. *Ecology*, *64*(5), 1249–1265. https://doi.org/10.2307/1937833

Nyssen, J., Pontzeele, J., & Billi, P. (2011). Effect of beaver dams on the hydrology of small mountain streams: Example from the Chevral in the Ourthe Orientale basin, Ardennes, Belgium. *Journal of Hydrology*, *402*(1), 92–102. https://doi.org/10.1016/j.jhydrol.2011.03.008

Panday, S., Huyakorn, P. S., Therrien, R., & Nichols, R. L. (1993). Improved three-dimensional finite-element techniques for field simulation of variably saturated flow and transport. *Journal of Contaminant Hydrology*, *12*(1–2), 3–33. https://doi.org/10.1016/0169-7722(93)90013-I

Phillips, J. V., & Tadayon, S. (2006). *Selection of Manning's roughness coefficient for natural and constructed vegetated and non-vegetated channels, and vegetation maintenance plan guidelines for vegetated channels in Central Arizona (Ser. Scientific investigations report 2006-5108)*. U.S. Department of the Interior, U.S. Geological Survey.

Salehin, M., Packman, A. I., & Paradis, M. (2004). Hyporheic exchange with heterogeneous streambeds: Laboratory experiments and modeling. *Water Resources Research*, *40*(11). https://doi.org/10.1029/2003WR002567

Savant, S. A., Reible, D. D., & Thibodeaux, L. J. (1987). Convective transport within stable river sediments. *Water Resources Research*, *23*(9), 1763–1768. https://doi.org/10.1029/WR023i009p01763

Sawyer, A. H., & Cardenas, M. B. (2012). Effect of experimental wood addition on hyporheic exchange and thermal dynamics in a losing meadow stream. *Water Resources Research*, *48*, W10537. https://doi.org/10.1029/2011WR011776

Sawyer, A. H., Cardenas, M. B., & Buttles, J. (2011). Hyporheic exchange due to channel-spanning logs. *Water Resources Research*, *47*(8). https://doi.org/10.1029/2011WR010484

Sear, D. A., Millington, C. E., Kitts, D. R., & Jeffries, R. (2010). Logjam controls on channel: Floodplain interactions in wooded catchments and their role in the formation of multi-channel patterns. *Geomorphology*, *116*(3), 305–319. https://doi.org/10.1016/j.geomorph.2009.11.022

Shahabi, A. A., Das, B. M. & Tarquin, A. J. (1984). *Empirical relation for coefficient of permeability of sand* (pp. 54–57). National Conference Publication, Institution of Engineers. Australia.

Spreitzer, G., Tunnicliffe, J., & Friedrich, H. (2020). Porosity and volume assessments of large wood (LW) accumulations. *Geomorphology*, *358*, 107122. https://doi.org/10.1016/j.geomorph.2020.107122

Therrien, R. (1992). *Three-dimensional analysis of variably-saturated flow and solute transport in discretely-fractured porous media Ph.D. Thesis*. Waterloo, Ont: University of Waterloo.

Therrien, R., & Sudicky, E. A. (1996). Three-dimensional analysis of variably-saturated flow and solute transport in discretely-fractured porous media. *Journal of Contaminant Hydrology*, *23*(1–2), 1–44. https://doi.org/10.1016/0169-7722(95)00088-7

Tonina, D., & Buffington, J. M. (2007). Hyporheic exchange in gravel bed rivers with pool-riffle morphology: Laboratory experiments and three-dimensional modeling. *Water Resources Research*, *43*(1). https://doi.org/10.1029/2005WR004328

Tonina, D., & Buffington, J. M. (2009). Hyporheic exchange in mountain rivers I: Mechanics and environmental effects. *Geography Compass*, *3*(3), 1063–1086. https://doi.org/10.1111/j.1749-8198.2009.00226.x

Trauth, N., Schmidt, C., Maier, U., Vieweg, M., & Fleckenstein, J. H. (2013). Coupled 3-D stream flow and hyporheic flow model under varying stream and ambient groundwater flow conditions in a pool-riffle system: Coupled 3-D stream flow and hyporheic flow model. *Water Resources Research*, *49*(9), 5834–5850. https://doi.org/10.1002/wrcr.20442

Trauth, N., Schmidt, C., Vieweg, M., Oswald, S. E., & Fleckenstein, J. H. (2015). Hydraulic controls of in-stream gravel bar hyporheic exchange and reactions. *Water Resources Research*, *51*(4), 2243–2263. https://doi.org/10.1002/2014WR015857

Valett, H. M., Dahm, C. N., Campana, M. E., Morrice, J. A., Baker, M. A., & Fellows, C. S. (1997). Hydrologic influences on groundwater-surface water ecotones: Heterogeneity in nutrient composition and retention. *Journal of the North American Benthological Society*, *16*(1), 239–247. https://doi.org/10.2307/1468254

van Gent, M. R. A. (1994). The modelling of wave action on and in coastal structures. *Coastal Engineering*, *22*(3–4), 311–339. https://doi.org/10.1016/0378-3839(94)90041-8

Ventres-Pake, R., Nahorniak, M., Kramer, N., O'Neal, J., & Abbe, T. (2020). Integrating large wood jams into hydraulic models: Evaluating a porous plate modeling method. *JAWRA Journal of the American Water Resources Association*, *56*(2), 333–347. https://doi.org/10.1111/1752-1688.12818

Wang, G.-T., Chen, S., Boll, J., Stockle, C. O., & McCooL, D. K. (2002). Modelling overland flow based on Saint-Venant equations for a discretized hillslope system. *Hydrological Processes*, *16*(12), 24092421. https://doi.org/10.1002/hyp.1010

Wilhelmsen, K. (2021). *Interacting Influence of log Jams and branching Channels on hyporheic exchange Revealed through laboratory Flume and numerical modeling experiments (Master's thesis)*. Retrieved from https://etd.ohiolink.edu/

Wohl, E. (2011). Threshold-induced complex behavior of wood in mountain streams. *Geology*, *39*, 587–590. https://doi.org/10.1130/G32105

Wohl, E. (2019). *Rivers in the Landscape* (2nd ed.). Wiley.

Wondzell, S. M., LaNier, J., Haggerty, R., Woodsmith, R. D., & Edwards, R. T. (2009). Changes in hyporheic exchange flow following experimental wood removal in a small, low-gradient stream. *Water Resources Research*, *45*(5). https://doi.org/10.1029/2008WR007214

Xu, M., Wang, Z., Pan, B., & Zhao, N. (2012). Distribution and species composition of macroinvertebrates in the hyporheic zone of bed sediment. *International Journal of Sediment Research*, *27*(2), 129–140. https://doi.org/10.1016/S1001-6279(12)60022-5

Xu, Y., & Liu, X. (2017). Effects of different in-stream structure representations in computational fluid dynamics models: Taking engineered log jams (ELJ) as an example. *Water*, *9*(2), 110. https://doi.org/10.3390/w9020110

Zarnetske, J. P., Haggerty, R., Wondzell, S. M., & Baker, M. A. (2011). Dynamics of nitrate production and removal as a function of residence time in the hyporheic zone. *Journal of Geophysical Research*, *116*(G1), G01025. https://doi.org/10.1029/2010JG001356

Zhang, Z.-Y., Schmidt, C., Nixdorf, E., Kuang, X., & Fleckenstein, J. H. (2021). Effects of heterogeneous stream-groundwater exchange on the source composition of stream discharge and solute load. *Water Resources Research*, *57*, e2020WR029079. https://doi.org/10.1029/2020WR029079

Zhou, T., & Endreny, T. A. (2013). Reshaping of the hyporheic zone beneath river restoration structures: Flume and hydrodynamic experiments. *Water Resources Research*, *49*(8), 5009–5020. https://doi.org/10.1002/wrcr.20384

Zhu, J., & Mohanty, B. P. (2002). Spatial averaging of van Genuchten Hydraulic parameters for steady-state flow in heterogeneous soils: A numerical study. *Vadose Zone Journal*, *1*, 12. https://doi.org/10.2113/1.2.261

References From the Supporting Information

Bear, J. (1972). *Dynamics of fluids in porous media*. New York, NY: American Elsevier.

El-Kadi, A. I., & Ling, G. (1993). The Courant and Peclet Number criteria for the numerical solution of the Richards Equation. *Water Resources Research*, *29*(10), 3485–3494. https://doi.org/10.1029/93WR00929

Elder, J. W. (1959). The dispersion of marked fluid in turbulent shear flow. *Journal of Fluid Mechanics*, *5*(04), 544. https://doi.org/10.1017/S0022112059000374

Fischer, H. B. (1965). Discussion of "numerical solution to a dispersion equation. *Journal of the Hydraulics Division*, *91*(2), 402–407. https://doi.org/10.1061/JYCEAJ.0001226

Fischer, H. B. (1968). *Methods for predicting dispersion coefficients in natural streams: With applications to lower reaches of the green and Duwamish rivers, Washington (ser. Dispersion in surface water)*. U.S. Govt. Print. Off.

Glover, R. E. (1964). *Dispersion of dissolved or suspended materials in flowing streams (Ser. Geological survey. professional paper, 433-b)*. U.S. Gov. Print. Off. https://doi.org/10.3133/pp433B

Guggenheim, E. A. (1954). The diffusion coefficient of sodium chloride. *Transactions of the Faraday Society*, *50*, 1048. https://doi.org/10.1039/tf9545001048

Jaiswal, S., Chopra, M., & Das, S. (2018). Numerical solution of two-dimensional solute transport system using operational matrices. *Transport in Porous Media*, *122*(1), 1–23. https://doi.org/10.1007/s11242-017-0986-x